# Numerical investigation of the combustion of liquid oxygen droplets in an environment of hydrogen under microgravity conditions

Mukund Gupta

A thesis

submitted in partial fulfillment of the

requirements for the degree of

Master of Science in Mechanical Engineering

University of Washington

2021

Committee:

Professor James C Hermanson

Professor John C Kramlich

Professor Alberto Aliseda

Program Authorized to Offer Degree:

Mechanical Engineering

University of Washington

## Abstract

Numerical investigation of the combustion of liquid oxygen droplets in an environment of hydrogen under microgravity conditions

Mukund Gupta

Chair of the Supervisory Committee:

Professor James Hermanson

Aeronautics & Astronautics

To develop more effective and better cryogenic powered liquid rocket engines, it is vital to undertake further studies to better understand the behavior of the LOX/$LH_2$ system. This work studies the configuration of a single liquid oxygen droplet surrounded by gaseous hydrogen diluted with helium. A numerical model using OpenFOAM as well as a coupled droplet evaporation model based on combining OpenFOAM results with the existing theoretical models have been developed to understand the species and temperature profiles near the droplet surface. The coupled droplet model estimates the droplet evaporation rate and droplet lifetime by achieving an energy balance between the calculated heat transfer from the flame to the latent heat associated with the simulated droplet evaporation. To reduce the computational complexity,

spherical symmetry is assumed while modelling the droplet, consistent with microgravity conditions.

OpenFOAM was employed to solve the conservation equations to calculate species concentrations and temperature profiles. Single-step, four-step, and six-step chemical reaction models were employed for simulating oxygen-hydrogen combustion. The global-chemistry reaction simulation was run until steady-state flame condition was achieved. Based on the numerical simulations for these chemical species, a blowing velocity of 0.0853 m/s for a fuel composition of 30% $H_2$ and 70% He was determined to be optimal parameters as it provides a solution to balancing the evaporation rate with the heat transfer. The temperature gradient was determined using the probe tool in Paraview. Using this as an input to the coupled droplet evaporation model developed using MATLAB, the mass balance equation was satisfied. The droplet lifetime was estimated using the $D^2$ Law. Suggestions are made based off these results for improving future simulation accuracy and efficiency.

# TABLE OF CONTENTS

# LIST OF FIGURES

# LIST OF TABLES

# NOMENCLATURE

μ: Dynamic viscosity

ρ: Density

υ: stoichiometric coefficient

$\mathcal{T}$: stress tensor

β: Temperature exponential of the modified Arrhenius equation

$\mathcal{D}$: Molar Diffusivity

$\alpha$: Heat diffusivity

$\partial_t$: Time derivative

$\hbar_j$: rate factor

$\bar{\rho}$: Molar Density

**u:** Velocity vector

*Sc*: Schmidt Number

*Pr*: Prandtl Number

*RR*: Reaction Rate

*A*: Arrhenius equation pre-exponential

*P*: Pressure

*R*: Source of specie density due to chemical interactions

*h*: Specific enthalpy (per unit mass)

$h_{f,m}$: Specific enthalpy of formation (per unit mass)

*X*: Mole Fraction

*Y*: Mass Fraction

*Ta*: Activation Temperature

$A_s$ : Sutherland coefficient

$T_s$: Sutherland Temperature

*Le*: Lewis Number

*rs*: radius of the droplet

$\dot{m}$: mass flow rate

$\widehat{C_p}$ : Molar specific heat

*M*: Molecular mass

$B_q$: Transfer number

*K*: Vaporization Constant

t: Time

$D_o$: Initial Droplet Diameter

*U*: Blowing Velocity

*Ar*: Area of the droplet

$k_g$: thermal conductivity

*C*: concentration factor

*c*: Specific heat

$\otimes$**:** Outer or cross product

$\boldsymbol{\nabla}$**:** Gradient

$\boldsymbol{\nabla}\cdot$ : Divergence

=

# ACKNOWLEDGEMENTS

First and foremost, I would like to thank Prof. James C Hermanson for providing me the opportunity to work on this research topic and for his research guidance, project direction, and draft edits that went into writing this thesis. This work would not have been possible without his constant motivation and his support. A special thank-you also goes to Florian Meyer and Dr. Christian Eigenbrod, our research collaborators at ZARM, Germany to their continued support and advise.

I would also like to extend my gratitude to my committee members Prof. Alberto Aliseda and Prof. John C Kramlich for agreeing to be on my thesis committee and for suggesting the necessary changes to enhance the quality of this thesis.

A special thank you to my undergraduate research mentor Dr. Ramalingam Senthil under whose guidance I really developed a passion for the field of academic research. My undergraduate research experiences under his supervision laid the solid foundation for me continue my passion in the field of thermofluids.

I would also like to thank David Wilson from AA Department for his constant support in with regards to troubleshooting the problems encountered during working on the server.

A special thank you also goes to my friends here in Seattle who became a family away from home and helped me navigate through the pandemic. Most notably, I would like to thank Sripathi, Shashank, Chaitanya, Alrick, Sumedh, Abhay Bohra, Niraj, Sairam, and Saransh. Without their support, encouragement, and help this thesis would not have been possible.

Finally, I would like to thank my parents, brother, grandmother, and other extended family members for their unconditional support, encouragement, and motivation despite being thousands of miles away without whom I would not have been successful.

# CHAPTER 1

# INTRODUCTION

## 1.1 LIQUID ROCKET PROPULSION

The bi-propellant liquid rocket utilizes fuel and oxidizer stored in separate tanks. The fuels and oxidizer are fed through a system of valves, pipes, and turbopumps to a combustion chamber where they combine and burn to produce thrust. Although liquid propellent rockets are more complex than solid propellant engines, they offer better tunability ensuring that the propellant flow can be controlled to the combustion chamber enabling the engine to be throttled, stopped, or restarted. However, the major benefit and reason behind studying the use of a liquid propellent rocket stems from its higher performance in comparison to the solid or hybrid rockets. Liquid Propellants employed in rockets are of three types: petroleum, cryogens, or hypergols [1]. In this work, cryogenic propellants, liquified gases stored at very low temperatures, are considered. A commonly used propellent is LOX/$LH_2$ which consists of liquid hydrogen as fuel and liquid oxygen as the oxidizer. This is also the system that has been used in this study. At the combustion chamber injector, oxygen typically remains in a liquid state at temperatures of -183$^o$C (-297$^o$F). In a typical spray combustion process, a mixture consisting of LOX droplets in $H_2$ occurs upon injection as $H_2$ is more likely to be pre-vaporized than $O_2$ due to the regenerative cooling of the rocket nozzle and hence it enters the combustion chamber in gas phase. Some of the advantages of using this system is high specific impulse and thrust levels required for space travel as well as producing harmless water as exhaust. High performance, low risk, and moderate cost of this fuel combination places $LH_2$-LOX as one of the most attractive rocket propellants for space-travel.

To achieve better effectiveness of future rocket engines using the liquid oxygen/hydrogen system a better understanding of the mixture formation, droplet vaporization, and resulting ignition and combustion is necessary. While some prior studies have been conducted on single LOX droplet vaporization under subcritical and supercritical conditions in a quiescent or convective $H_2$ environment, few numerical models have been developed and validated with experimental data to completely understand the combustion behavior of the LOX droplet. Through this research, an effort has been made to answer some of these questions by developing a numerical model for the combustion of LOX droplet under cryogenic conditions and validate it with the experimental data obtained from collaborators at ZARM, Germany. The experiment that motivates the current numerical study is discussed briefly below.

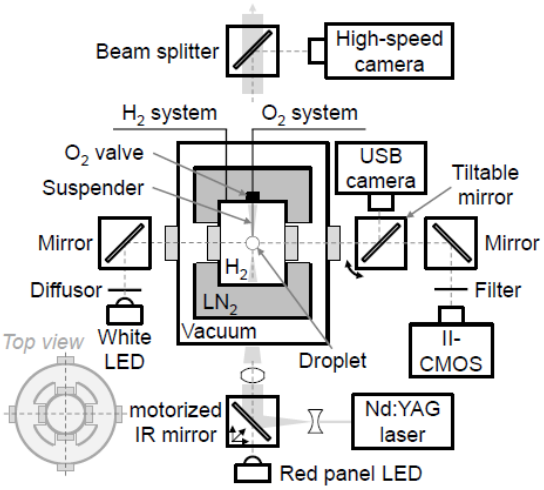


Figure 1.1: Experimental setup for the schematic of the combustion chamber diagnostics [2].

The experiments are performed under microgravity conditions at the ZARM drop tower facility located at the University of Bremen in Bremen, Germany. The drop tower offers the microgravity quality of $10^{-6}$ g for a test duration of 4.9 s. Testing in a microgravity environment allows the use of larger droplets (in the size of mm rather than μm) and is advantageous as it enables great simplification of the experimental results as well allowing the use of well-established diagnostic techniques to study the combustion behavior of liquid oxygen droplets. Fig. 1.1 shows the

experimental setup and various diagnostic systems used to study the LOX droplet combustion. The setup consists of a combustion chamber containing the LOX droplet and $H_2$ gas surrounded by liquid-nitrogen cooling jacket, which is then surrounded by a vacuum container that provides the necessary thermal isolation. The combustion chamber is cooled to a fixed temperature of 77 K and the combustion chamber is connected to a gaseous supply of pure $H_2$. The liquid oxygen droplet enters onto the suspender tip within the combustion through a valve mounted on the top of the combustion chamber. The droplet is ignited within the combustion chamber through the pulsed Nd:YaG laser [2].

A total of 16 drop-tower experiments have been performed to date at the ZARM facility in the pressure range of 1-45 bar. All the experiments were performed in 100% $H_2$ atmosphere. From the experiment, the droplet lifetime was determined to be 136.5 ms. During the experiments, it was observed that an ice shell is formed near the droplet surface, and this can be observed by the change in droplet shape at low pressures and this effect appears to decrease significantly at pressures greater than 20 bar. At the end of the combustion process, it is observed that droplet begins to rotate and turn. Additionally, small jets consisting of gaseous oxygen appear from the droplet surface leading to the phenomenon of micro explosions. It has been found that burning constant increases with an increase in pressure [2]. These experimental results provide baseline cases for comparing the numerical results of the current study.

## 1.2 LIQUID OXYGEN DROPLET COMBUSTION PROCESS

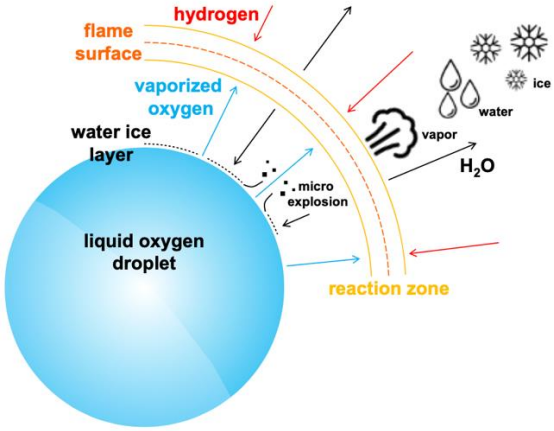


Figure 1.2: Liquid Oxygen Droplet Combustion [2-4]

Figure 1.2 shows the liquid oxygen droplet combustion process and highlights the various chemical and physical processes observed during the droplet combustion. These processes are complex and not all of them are addressed in the current modeling effort, which focuses on the computed flame zone and the simulated droplet vaporization.

At the reaction zone of the flame, both the liquid hydrogen and liquid oxygen react. Gaseous hydrogen is transported from the outside while the vaporized oxygen is transported from the inside to the reaction zone. This reaction can be considered droplet combustion "in reverse," where the droplet consists of oxidizer and the "air" is actually the fuel. Near the flame zone, water vapor is formed which cools down in the cryogenic surrounding. Owing to this environment, the water vapor formed might either condense or freeze. A water-ice layer is likely formed on the liquid oxygen droplet as the water vapor reaches the droplet surface. Small micro-explosions are then possible when oxygen breaks through the ice layer which could in turn cause stronger directional changes as the droplet mass decreases and produce the observed droplet motion. The effects described of a possible icing of the droplet surface can be observed by the change in droplet shape, especially at low pressures, and this effect appears to decrease at higher pressures (>20 bar).

Nevertheless, individual ice particles remain after the end of combustion even at high pressures. These effects have been suggested by the ZARM results to date.

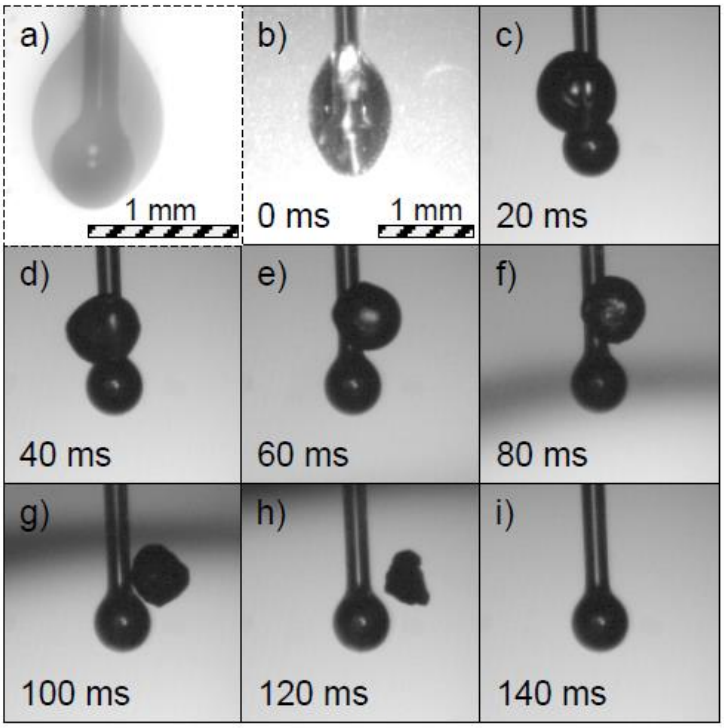


Figure 1.3: High-speed shadowgraph images of the LOX/$LH_2$ combustion at P=1 bar. [2]

Figure 1.3 highlights the LOX droplet combustion behavior observed experimentally. Once the droplet at the suspender tip is ignited by a laser spark, it begins to detach itself from the suspender tip after a time period of 20-50 ms. The droplet is initially elliptical at the suspender tip due to good wettability properties of the LOX on the quartz suspender but takes on a spherical shape once detached from the suspender tip. The experiments also observe the phenomenon highlighted in Fig. 1.2. There have been instances of micro-explosions, ice formation, and water ice layer formation that have been reported. Additionally, condensation of water vapor is observed at higher pressures [2].

In this work, a numerical model is developed to study the flame surface/ reaction zone as shown in Fig. 1.2. Other observable physical effects such as micro-explosions, ice formation, and water ice layer formation are not considered here. The flame zone can be modelled as a counterflow flame diffusion in which the $O_2$ gas supplied from the one of the boundaries which represents the inflow of oxygen resulting from the droplet vaporization. The $H_2$ gas is supplied from the other boundary, and this reacts with the $O_2$ gas according to the specified chemistry scheme. Finally, the major species concentration profile and flame temperature profiles have been determined.

## 1.3 GOALS AND OBJECTIVES

To achieve the numerical modelling liquid oxygen droplet combustion in gaseous hydrogen, the following goals and objectives were identified:

- Establish and evaluate the capability of OpenFOAM to model hydrogen/oxygen combustion under the cryogenic conditions of this investigation.
- Use OpenFOAM to determine the temperature profile and major species profiles under steady-state conditions.
- Couple the OpenFOAM results with an analytical model that simulates the evaporation of liquid oxygen at the droplet surface.
- Use the coupled analytical model that utilizes the results of temperature profile from OpenFOAM and input that into a theoretical model that estimates the droplet vaporization rate, droplet lifetime and plots the $D^2$ Law

The following chapters will introduce in more detail the numerical modelling, results, the main findings of this work and offer some recommendations to address the future scope of this work.

# CHAPTER 2

# NUMERICAL MODELLING

A numerical model based on conservation equations is utilized to capture the dynamics of droplet combustion.

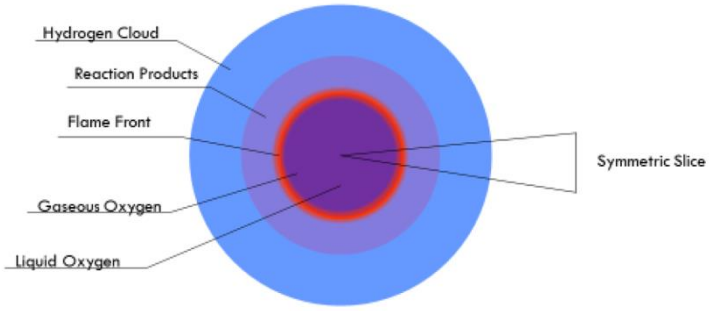


Figure 2.1: Droplet Combustion Domain [5]

The spherically symmetric geometry of the problem modeled here is shown in Fig. 2.1. For the purposes of these simulations the liquid droplet is replaced with an equivalent volume of gaseous oxygen, providing a source of oxygen vapor that simulates the evaporation rate of the liquid. In this work, three different approaches have been used to achieve the numerical modelling. The first approach involves using reactingFoam solver of OpenFOAM suite. A second approach involves usage of a droplet model which uses the energy balance between the results of theoretical values and the OpenFOAM simulations to match the heat flux due to evaporation to the heat conduction to the simulated droplet surface. The third approach involves usage of OpenSMOKE++ solver developed at CRECK Modelling Group at Politecnico Di Milano. Each of these approaches are explained in detail in the following sections.

## 2.1 OpenFOAM

In lieu of developing in-house software, the open source OpenFOAM platform has been used for all flame-zone modelling [6,7]. “Open-source Field Operation and Manipulation” (OpenFOAM) is an open-source and free software developed by OpenCFD Limited. OpenFOAM

uses C++ programming language and is designed to run on Linux systems. OpenFOAM is highly object oriented and this enables the users to introduce new solvers without changing the main source code. To solve complex fluid dynamics problems, OpenFOAM uses the Finite Volume Methodology (FVM) over a collocated grid arrangement. This enables OpenFOAM to store all dependent variables at the cell location which minimizes the computational effort. The opensource licensing of OpenFOAM allows the users to contribute their codes to the OpenFOAM community and help in expanding the ever-increasing library. OpenFOAM software package allows users a package to solve various differential equations ranging from lagrangian particle dynamics to Finite Element Analysis (FEA). Owing to its vast library with each solver having its own unique capability of solving multi-physics problems, each solver can be used to solve varying problems and have a specific implementation to the fluid dynamics problem. The overall working structure of OpenFOAM is shown in Fig. 2.2.

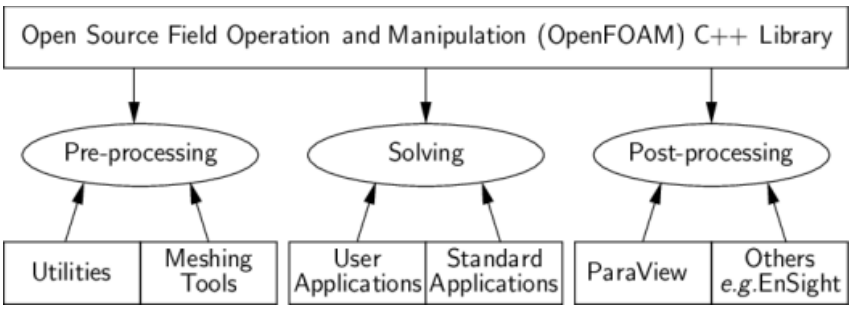


Figure 2.2: Overall Structure of OpenFOAM [6]

As with any CFD solver, OpenFOAM has three main parts: pre-processing, solving, and post-processing. Pre-Processing tool allows the user defines the mesh, initial and boundary conditions, and fluid properties. Through the solver, OpenFOAM solves the specified equations by discretizing it using the mathematical scheme specified by the user. Finally, the post-processing tool is used to visualize the simulation and plot the results.

OpenFOAM has the following advantages: No license cost, highly object oriented, fully documented source code, and ease of writing partial differential equations. It also has the following disadvantages: Lack of graphical user interface which necessitates the separate installation of paraview software for the visualization of the results. OpenFOAM could also prove to be a challenge to use for the user unacquainted with non-visual, command line environment. Furthermore, the C++ structure of OpenFOAM code requires a lot of memory to run. The lack of proper documentation for some of the solvers used in OpenFOAM could also prove to be a challenge for someone not well versed with the course of numerical methods. As OpenFOAM is an opensource software which is constantly getting added with more features, there will be situations where one version of OpenFOAM might behave very different from the other version of OpenFOAM due to the implementation of better numerical schems. More details on OpenFOAM can be found in OpenFOAM User Guide [6,7].

The reactingFoam model serves as the basis to simulate the droplet combustion behavior as it incorporates the multiphase fluid mechanics with chemical interactions. reactingFoam solver's case of counterFlowDiffusion2D flame has been used to achieve the numerical modelling for this study. For this solver, the mandatory input fields required are $p$ (pressure), $U$ (velocity), and $T$ (Temperature).

## 2.2 ASSUMPTIONS MADE FOR NUMERICAL MODELLING

The following assumptions have been made to reduce the computational complexity of the model and to effectively reduce the model from a 3D case to a 1D case:

1. The droplet region and the overall configuration are both spherically symmetric. This is an idealization appropriate for modelling the droplet geometry in microgravity conditions.

2. The overall process is quasi-steady. The profiles of major species concentration and flame temperatures can only be determined once the quasi-steady solution has been achieved and the ignition transients are not considered.
3. Effects of radiation and turbulence are not considered. Since hydrogen/oxygen flames are not highly luminous, effects of radiation is neglected. Also, there is no convective flow so there is no shear potentially leading to flow turbulence.
4. Chemistry (i.e., the chemical reaction schemes) is fast, which leads to a compact flame zone. In this work, several different chemistry schemes have been implemented.
5. There is no convective flow in the computational domain, and no motion of the droplet relative to the surrounding gas. This is appropriate for an isolated droplet under zero-g conditions.
6. Surface Tension is neglected as the droplet is simulated as pure vapor, and there is no actual droplet/vapor interface
7. Uniform properties inside the droplet are assumed
8. No fluid motion inside the droplet is considered
9. Ideal gas properties are assumed for all species. This is an excellent assumption for hydrogen gas and a good approximation for oxygen gas and water vapor near the flame front. Experiments have however reported saturation/freezing far from the flame and near the droplet surface.

## 2.3 GOVERNING EQUATIONS

This section lists the governing equations that are essentially partial differential equations that drive the mass, energy, momentum, and species transport within the described computational domain. These are the foundational equations solved by OpenFOAM:

### *2.3.1 Conservation of Mass*

The equation satisfying the governing equation for conservation of mass is the standard continuity equation. Under the steady state solution, the non-stationary term disappears, which this leads to the equation 2.1 shown below where $\rho$ is the bulk density and $\mathbf{u}$ is the velocity vector.

$$\partial_t \rho + \boldsymbol{\nabla} \cdot (\rho \mathbf{u}) = 0 \tag{2.1}$$

### *2.3.2 Conservation of Momentum*

The governing equation used by reactingFoam for the conservation of momentum is given by equation 2.2 where $\mathbf{u}$ is the velocity vector, $\rho$ is the bulk density, P is the pressure, and $\mathcal{T}$ is the deviatoric stress tensor.

$$\partial_t(\rho \mathbf{u}) + \boldsymbol{\nabla} \cdot (\rho \mathbf{u} \otimes \mathbf{u}) = -\boldsymbol{\nabla} \cdot \mathrm{P} - \boldsymbol{\nabla} \cdot \mathcal{T} \tag{2.2}$$

The simulations that are run in this work assume a uniform pressure across the entire computational domain. Therefore, the term $\boldsymbol{\nabla} \cdot \mathrm{P}$ in the equation 2.2 becomes zero. For a Newtonian fluid, the deviatoric stress tensor is given by the equation 2.3.

$$\boldsymbol{\nabla} \cdot \mathcal{T} = \boldsymbol{\nabla} \cdot [\mu(\boldsymbol{\nabla}\mathbf{u} + (\boldsymbol{\nabla}\mathbf{u})^T)] + \boldsymbol{\nabla}[\frac{2}{3}\mu\,(\boldsymbol{\nabla} \cdot \mathbf{u})] \tag{2.3}$$

where $\mathbf{u}$ is the velocity vector and $\mu$ is the dynamic viscosity. Ideally, the value of deviatoric stress tensor should be zero because of the assumed condition of no shear. However, it is not possible to verify this as the viscosity is determined within the reactingFoam model using the Sutherland

model and is not provided as an input. The phenomenon of Stefan flow is expected during the LOX droplet combustion process and during the experiments. This is especially relevant during the simulated mass flow from the droplet surface due to the vaporization.

*2.3.3 Species Conservation*

The governing equation used by reactingFoam for the conservation of species is given by equation 2.4 where $Y_i$ is the species mass fraction, $\rho$ is the bulk density, $\mathcal{D}_i$ is the molar diffusivity, and $R_i$ is the chemical source term.

$$\partial_t(\rho Y_i) + \nabla \cdot (\rho Y_i \mathbf{u}) - \underbrace{\nabla \cdot [\mathcal{D}_i \nabla(\rho Y_i)]}_{Diffusive\ Transport} = \underbrace{R_i}_{chemical\ source} \tag{2.4}$$

Determining the molar diffusivities in a multi-component mixture is difficult and complex. It is not possible to determine precisely how OpenFOAM computes the species diffusivities as it is done in the reactingFoam solver blackbox. A good estimate for determining molar diffusivities in reactingFoam is through the use of unity Schmidt's number assumption in reactingFoam. For a specie $i$, diffusivity $\mathcal{D}_i$ can be approximated using a unity Schmidt number:

$$Sc_i = \frac{\upsilon}{\mathcal{D}_i} \cong 1 \ , \tag{2.5}$$

which implies, $\upsilon = \mathcal{D}_i$ .

ReactingFoam uses Sutherland model to determine the viscosity of the component. The Sutherland model determines the value of viscosity as a function of Temperature from the Sutherland coefficient $A_s$ and Sutherland Temperature $T_s$. More information on this can be found using OpenFOAM user guide [6].

The Reaction rate of each species can be computed as follows:

$$RR_j = \kappa_j \prod_{m}^{N_{species}} {C_m}^{\upsilon_{j,m}} \quad , \tag{2.6}$$

where $\kappa_j$ is the rate factor, $C_m$ is the concentration factor of the species, and $\upsilon_{j,m}$ is the stoichiometric coefficient of the species.

The reaction rate can be computed using the rate factor, $\kappa_j$, and the concentration factors. The rate factor is determined through the modified Arrhenius equation:

$$\kappa_j = A_j \, T^{\beta_j} e^{-\frac{T_{a,j}}{T}} \quad , \tag{2.7}$$

where $A_j$ is the Arrhenius equation pre-exponential, $\beta_j$ is the temperature exponential of the modified Arrhenius equation, and $T_{a,j}$ is the activation temperature.

The value of $R_i$ can be computed as follows:

$$R_i = -\sum_{j}^{N_{reac}} \upsilon_{i,j} RR_j \quad , \tag{2.8}$$

where *RR* is the reaction rate and $\upsilon_{j,m}$ is the stoichiometric coefficient of the species. *R* is the chemical source term in the equation 2.4 and is the sum of the product of stoichiometric coefficients and reaction rates for the all species present within the computational domain.

### 2.3.4 *Conservation of Energy*

Equation 2.9 below represents the governing equation satisfying the law of conservation of energy where *h* represents the value of enthalpy, **u** is the velocity vector, $\rho$ is the bulk density, $\mathcal{K}$ is the thermal conductivity, *T* is the temperature and $\dot{Q}_{reac}$ is the heat of reaction.

$$\partial_t \left(\rho h + \frac{1}{2}\rho|\boldsymbol{u}|^2\right) + \boldsymbol{\nabla}\cdot\left(\rho\mathbf{u}(\mathrm{h} + \frac{1}{2}|\boldsymbol{u}|^2\right) - \partial_t\rho - \boldsymbol{\nabla}\cdot(\mathcal{K}\,\boldsymbol{\nabla}T) = \dot{Q}_{reac} \tag{2.9}$$

Under the assumption of unity Prandtl number, the thermal conductivity $\mathcal{K}$ of the fluid can be approximated:

$$Pr = \frac{\upsilon}{\alpha} \approx 1 \ , \tag{2.10}$$

which implies, $\mathcal{K} = C_p\mu$.

While an assumption of unity Prandtl number is reasonable, it is not possible to vary the Prandtl number parameter in OpenFOAM. As stated in the assumptions, the effects of radiation and viscous dissipation are accounted for in the numerical study, $\dot{Q}_{reac}$ in this case only accounts for the chemical reaction and does not include any external heat input.

The value of $\dot{Q}_{reac}$ can be computed as follows:

$$\dot{Q}_{reac} = \sum_{j}^{N_{reac}} (\, RR_j \sum_{m}^{N_{species}} \upsilon_{j,m} h_{f,m}\,) \ , \tag{2.11}$$

where *RR* is the reaction rate, $\upsilon_{j,m}$ is the stoichiometric coefficient of the species and $h_{f,m}$ is the specific enthalpy of formation (per unit mass) of the species.

## 2.4 EQUATIONS OF STATE

For a closure problem, it is necessary to describe the equations of state as these equations link the different conservations laws with each other. All the species used for describing the equations of state are assumed to be ideal gas. This is an excellent approximation for gaseous hydrogen under the current simulation conditions as oxygen moves further away from the droplet

as it heats up and vaporizes. This approximation is also valid for water vapor in the vicinity of the flame zone but will not hold true very near the droplet surface for oxygen, nor near the droplet surface or in the far field for water vapor. The equation of state model is specified within the thermophysical modelling library of the OpenFOAM framework. The value of the specific heat at constant pressure, *Cp*, for each species is specified in the thermodynamics sub dictionary of the Thermophysical property data file in the form of high *Cp* Coefficients and low *Cp* coefficients from the JANAF thermodynamics table. These thermodynamic models are used to calculate the value of *Cp* from which all other properties are derived. The values of these coefficients and other thermophysical data are determined using the NIST database [8]. Once these values are specified, OpenFOAM would then estimate the $c_p$values at all the cell locations within the computational domain. The energy sub dictionary of the *thermoType* dictionary file used is *sensibleEnthalpy*. The following equations of state have been used in this work:

$$P = \bar{\rho} R_u T \tag{2.12}$$

$$\bar{\rho} = \rho \sum_{i}^{N_{species}} \frac{Y_i}{M_i} \tag{2.13}$$

$$h = h_f + \int c_p \, T \tag{2.14}$$

## 2.5 CHEMISTRY SCHEMES

The combustion of liquid oxygen with hydrogen produces a number of species, only 8 species appear in measurable quantities. [9]. They are:

- $H_2$: Hydrogen

- $O_2$: Oxygen
- H: Hydrogen radical
- O: Oxygen radical
- OH: Hydroxyl radical
- $H_2O_2$: Hydrogen Peroxide
- $HO_2$: Hydroperoxyl radical

The combustion processes include a number of reaction steps. In this work, three chemistry schemes have been tested namely one-step chemistry, four-step chemistry, and six-step chemistry. The rationale behind this was to find out which chemistry scheme was able to model the combustion properly without being too computationally expensive. In all of these chemistry schemes, helium gas is introduced as a diluent to the hydrogen as the results obtained by running the simulations in 100% $H_2$ were impractical especially for temperature profiles where the differences between the theoretical and simulated values were greater than 1000 K. Lewis number is computed as the ratio of Schmidt number and Prandtl number. Since both Schmidt number and Prandtl number are assumed to be unity in OpenFOAM, the Lewis number of all the species is assumed to be unity in reactingFoam. Also, at these high concentrations of $H_2$ the major species profiles also become unphysical presumably due to the unity Lewis number assumption in OpenFOAM which makes the species diffusion of $H_2$ at higher concentration unphysically fast and this causes the deviations in species concentration and temperature profiles at these higher concentrations. This unity Lewis number assumption for $H_2$ forces the $H_2$ diffusion to be unrealistically fast and this leads to high flame temperatures (mention why). Hydroperoxyl radical and Hydrogen Peroxide are negligible in all of the chemical schemes considered here.

### (i) SINGLE-STEP CHEMISTRY

The single step chemistry model used was obtained from Lawrence Livermore National Lab, CA [10]. This chemistry scheme consists of one chemical reaction and three participating species. A single-step chemistry scheme was tried as it offered the advantages of being a simple and less computationally expensive chemistry scheme. The unrealistic flame temperatures obtained as well as the unreasonable species concentrations are the major disadvantages of this scheme. The rate coefficients for the single-step chemistry model are given in Table 2.1

| Reaction | A | Ta | β |
|---|---|---|---|
| $H_2 + \frac{1}{2}O_2 \Rightarrow H_2O$ | 1.8e13 | 17614 | 0 |

Table 2.1: Single Step Chemistry model

### (ii) FOUR-STEP CHEMISTRY

The four-step chemistry model used was obtained from Forman William's Group at University of California, San Diego [11]. This chemistry scheme consists of four chemical reactions and six chemical species. The reason behind attempting this scheme was to determine whether the four-step chemistry models the droplet combustion behavior as effectively as the six-step chemistry but at a reduced computational cost. Overall while running the simulations, the four-step chemistry did not represent a major computational improvement in comparison to the six-step chemistry discussed next. Moreover, the four-step chemistry could not be modelled properly owing to the lack of the availability of the values of A, Ta, and β in the literature. The reactions in the four-step chemistry model are given in Table 2.2; here the rate constants were taken to be those of the six-step model discussed below.

| Reaction |
|---|
| $H + O_2 \Rightarrow OH + O$ |
| $O + H_2 \Rightarrow OH + H$ |

| $OH + H_2 \Rightarrow H_2O + H$ |
| --- |
| $2H \Rightarrow H_2$ |

Table 2.2: Four Step Chemistry model

### (iii) SIX-STEP CHEMISTRY

The six-step chemistry model was obtained from Yetter & Glassman [9]. This chemistry scheme consists of six chemical reaction and six participating species. The following reactions are a part of a full 21 reaction model and selected based off their roles of chain-initiation, chain-branching, and chain-termination. The following steps represent the chain initiation, chain-propagation, and chain-terminating steps.

- The Chain Initiating:

$$H_2 \Longrightarrow 2H$$

- Chain Propagating:

$$H + O_2 \Longrightarrow O + OH$$

$$O + H_2 \Longrightarrow H + OH$$

$$H_2 + OH \Longrightarrow H + H_2O$$

- Chain Terminating

$$2O \Longrightarrow 2H$$

$$H + OH \Longrightarrow H_2O$$

The reason for choosing six step chemistry scheme is because it offers a good approximation of the flame temperature, estimating the heat transferred to the droplet and major species concentration profile. The goal of this work is to focus primarily on the major species and temperature profiles than on the minor species concentrations. Using a six-step chemistry helps in achieving this goal. The rate coefficients for the six-step chemistry model are given in Table 2.3.

| Reaction | A | Ta | β |
|---|---|---|---|
| $H + O_2 \Rightarrow OH + O$ | 3.55e15 | 8353 | -0.4 |
| $O + H_2 \Rightarrow OH + H$ | 5.08e04 | 3166 | 2.7 |
| $H_2 \Rightarrow 2H$ | 4.58e19 | 52530 | -1.4 |
| $H + OH \Rightarrow H_2O$ | 3.80e22 | 0 | -2.0 |
| $2O \Rightarrow O_2$ | 6.16e15 | 0 | -0.5 |
| $OH + H_2 \Rightarrow H_2O + H$ | 2.16e08 | 1726 | 1.5 |

Table 2.3: Six Step Chemistry Model

## 2.6 COMPUTATIONAL DOMAIN

Once the numerical scheme to solve the governing equations and the chemistry schemes are identified, the next step is to specify the computational domain. Fig. 2.3 shows the finite volume mesh that has been used for the computational domain.

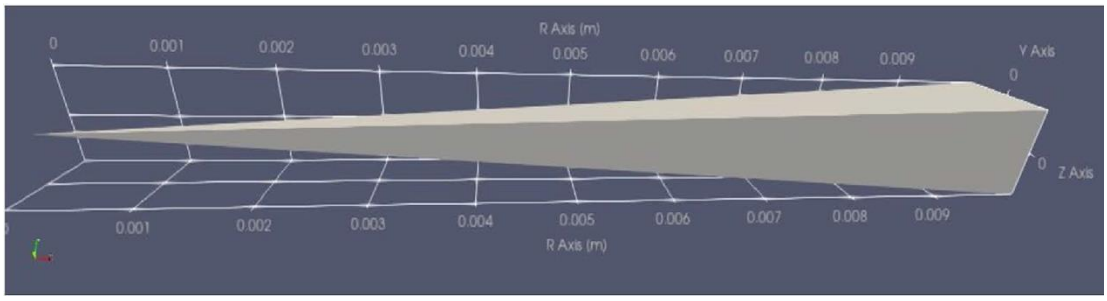


Figure 2.3: Geometry of the computational domain

The oxygen is introduced into the computational domain in gas phase; the vaporization of liquid oxygen at the droplet surface is not modeled directly. The computational grid consists of a wedge modeling a segment of the spherically symmetric geometry. The computational domain consists of 10,000 mesh cells over physical extent ranging from 0.5 mm (the simulated droplet boundary) to 20 mm at the outer (hydrogen-side) boundary. Conservation equations are solved for every point in the computational domain. The computational mesh was constructed in OpenFOAM's blockMesh tool using a linearly increasing cell size. The meshed computational

domain is shown in Fig. 2.4. All simulations were run for a pressure of 1 bar and an initial temperature of 100 K. The temperature was fixed at the oxygen-inlet boundary; for the external (hydrogen side) boundary, an adiabatic-wall condition or isothermal-wall condition was applied. Also, there is no outflow at the hydrogen side (outer) boundary of the domain. The flow velocity or the blowing velocity at the oxygen side boundary (inner boundary) was variable.

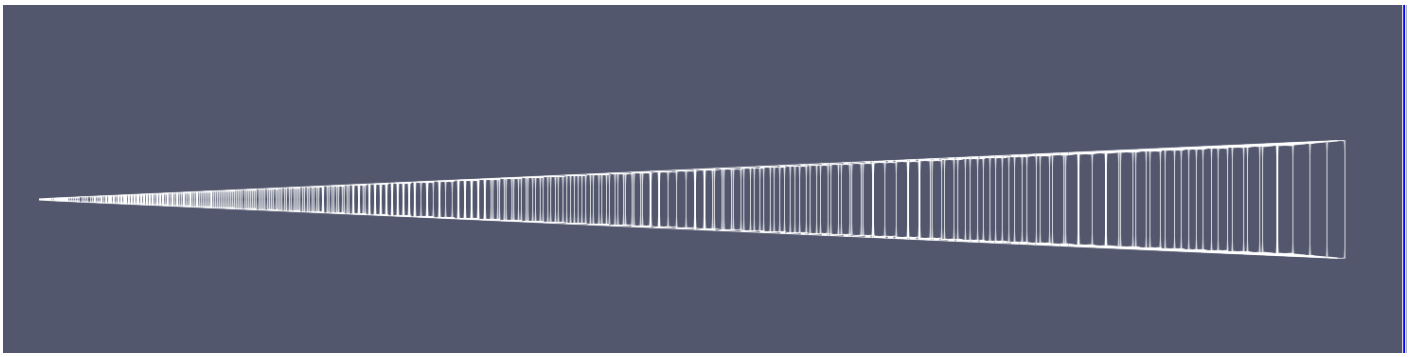

Figure 2.4: Snapshot of finite-volume mesh of the computational domain

**2.7 PIMPLE ALGORITHM**

The reactingFoam solver in OpenFOAM uses a PIMPLE algorithm to solve the governing equations. PIMPLE algorithm combines the following two algorithms: Pressure Implicit with Splitting of Operators (PISO) and Semi-Implicit Method for Pressure Linked Equations (SIMPLE). Fig 2.5 represents the flow-chart of various steps taken by the PIMPLE algorithm. The PIMPLE algorithm is used once the continuity equation is solved. The reactingFoam solver is based on the equations of continuity, momentum, species transport, and energy equations. Doubani [12] provides more information about how these conservation equations are solved within the reactingFoam model. Species, energy, and velocity are entered into the solver as header files which are solved within the chemistry loop as shown in the Fig. 2.5.

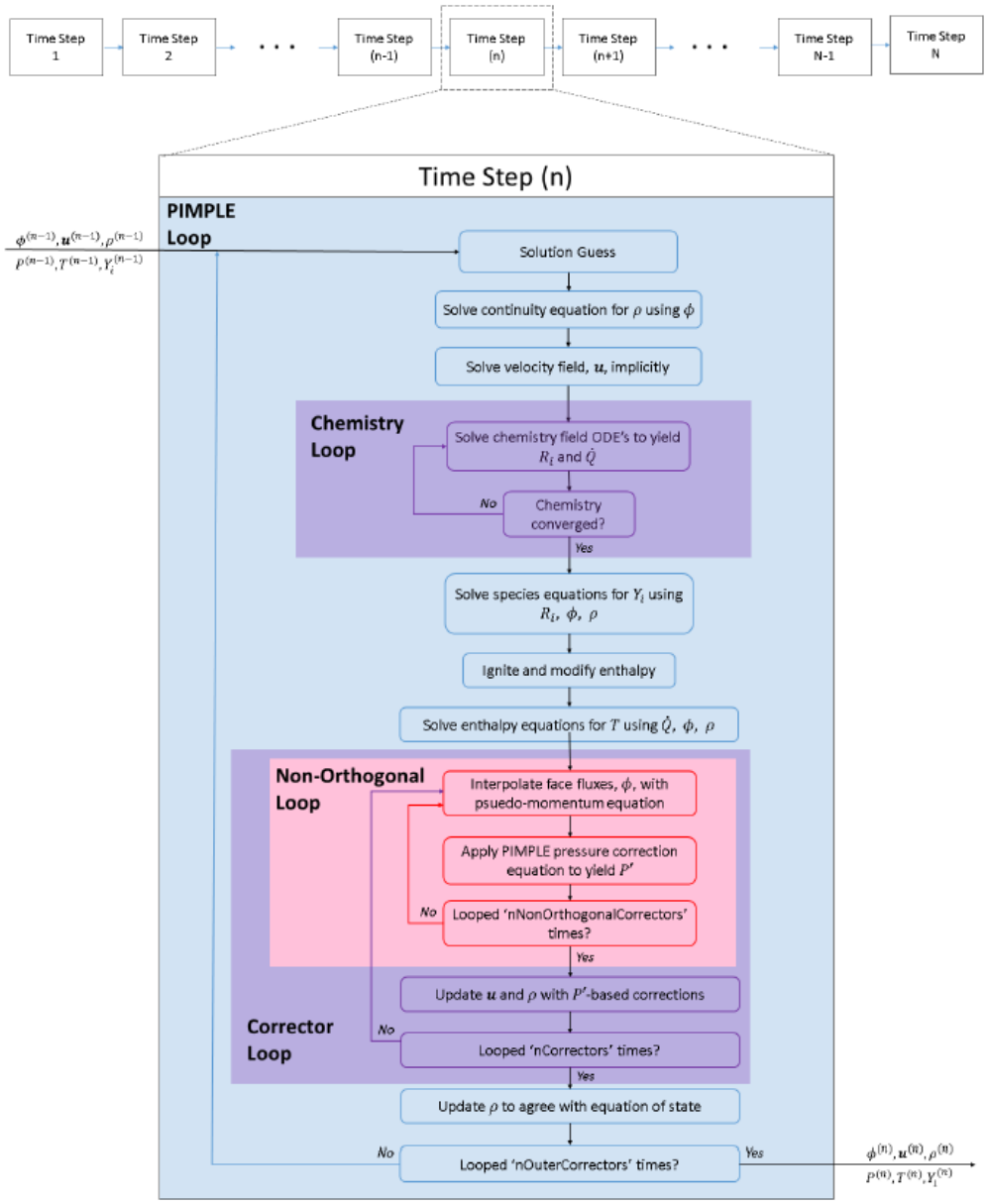


Figure 2.5: Steps taken in the PIMPLE algorithm [13]

## 2.8 IGNITION

After a suitable interval of inter-diffusion of the gaseous oxygen and hydrogen, combustion is initiated by an assumed temperature profile. Figure 2.6 shows this assumed temperature profile. The numerical modeling in this work has considered as a nominal case pure oxygen reacting with a mixture of 30% hydrogen in 70% helium by volume. This approach of using a superimposed

temperature profile to get the necessary combustion behavior was adopted after identifying the limitations associated with using a spark ignition method. Specifically, Frydman [13] reports that a major limitation associated with using a spark ignition method is the value of high flame temperature and enthalpy that were obtained. The flame temperatures obtained using this approach were off by a value of 1500 K from the theoretical values. Also, the heat released obtained using this approach were much higher owing to the artificial spark that has been used to ignite the mixture.

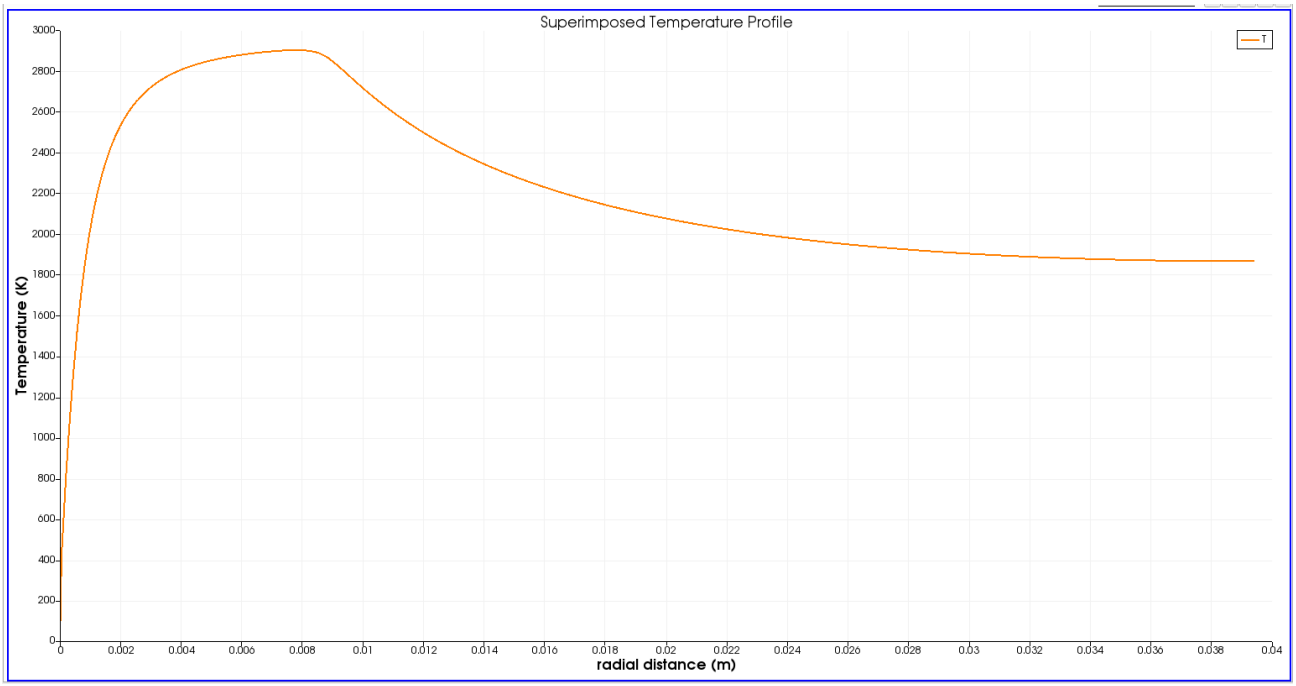


Figure 2.6: Assumed Temperature profile

## 2.9 MODELING DROPLET EVAPORATION

A phenomenological model combining the simulated droplet evaporation rate using a MATLAB code to the flame result from the OpenFOAM was implemented, as described below.

The rate of vaporization at the liquid droplet surface can be estimated by relating the conductive heat flux from the flame (there is no convection in zero-g) to the inflow of gaseous oxygen provided at the oxygen side of the computational domain. The underlying relationship is shown in Eq. 2.15:

$$\underbrace{k_g \cdot \underbrace{\frac{\partial T}{\partial r}}_{OpenFOAM\ simulation} \cdot A}_{} = \underbrace{\dot{m} \bullet h_{vap}}_{Theory} \quad , \tag{2.15}$$

where $k_g$ is the thermal conductivity of the vapor in the vicinity of the oxygen interface, $\frac{\partial T}{\partial r}$ is the radial temperature gradient in the immediate vicinity of the simulated droplet surface, $\dot{m}$ the mass flow of the gaseous oxygen, and $h_{vap}$ the latent heat of vaporization for oxygen and *A* is the area. Under the simplifying assumptions of quasi-steady evaporation, uniform droplet temperature, and binary diffusion with unity Lewis number (no hydrogen present on the droplet side of the flame), and constant thermal properties, this relation can be further developed [14] to develop this relation for the mass flowrate.

$$\dot{m} = \frac{4\pi k_g r_s}{c_{pg}} \ln\left(B_q + 1\right) \quad , \tag{2.16}$$

where $c_{pg}$ is the specific heat capacity of the vapor in the vicinity of the droplet surface and $B_q$ is the transfer number and $r_s$ is the droplet radius.

Adjusting the value of the transfer number allows matching the vaporization rate given by Eq. 2.16 with the rate of heat transfer from the quasi-steady state flame configuration obtained from OpenFOAM using Eq. 2.15. This matching is done in an iterative fashion, where the transfer number specifies a vaporization rate, which prescribes the gaseous oxygen inflow boundary condition into the numerical OpenFOAM solution. This inflow is then adjusted iteratively until

the heat flux due to the simulated vaporization is matched by the heat conduction from the flame as determined from OpenFOAM. The resulting solution thus specifies the reactant consumption rates, which ultimately relate to to the droplet lifetime using the familiar d-squared law, which has been verified by the experiments [2].

The heat input at the location of the simulated oxygen droplet region is computed from the temperature profile in the flame, using a thermal conductivity for the gas mixture near the droplet estimated using methods outlined in Bird *et al.* [15]. The value of $k_g$ is computed using the formula specified by Bird *et al.* [15]:

$$k_g = \left(\widehat{C_p} + \frac{5}{4}\frac{R}{M}\right)\mu \tag{2.17}$$

The vaporization constant K is determined using the following equation specified in Turns [14]:

$$K = \frac{8k_g}{c_{pg}\rho_l}\ln\left(B_q + 1\right)\ , \tag{2.18}$$

where $\rho_l$ is the density of the liquid state. An iterative solution was performed by varying the transfer number $B_q$, and hence the oxygen blowing velocity, until the heat sink at the simulated droplet surface due to the oxygen mass flow and heat of vaporization matched the conductive heat transfer from the flame, satisfying Eq. 2.15.

Following the calculation of K, the equation of $D^2$ Law can be computed as follows [14]:

$$D^2(t) = D_o^2 - Kt\ \ , \tag{2.19}$$

where $D_o$ represents the initial droplet diameter and t represents the time for which the droplet combustion experiment is carried out.

The droplet lifetime is then estimated using the formula given below [14]:

$$t_d = \frac{D_o^2}{K} \tag{2.20}$$

# CHAPTER 3

# RESULTS

This chapter reports the results that were obtained when the numerical simulations were run for single step, four step, and six step chemistry schemes. It also reports the results obtained while running simulations in OpenFOAM and for the coupled droplet evaporation model. For the simulations made in OpenFOAM, the plots of the temperature and molar concentration profiles were made using Paraview data-visualization program. The coupled model was written in MATLAB and the $D^2$ Law was also plotted using MATLAB.

An important consideration in determining the effectiveness and limitations of OpenFOAM in modeling the combustion is how well the solutions conform to the expected adiabatic flame temperatures for the hydrogen/oxygen reaction for various amounts of helium dilution of the fuel. Table 3.1 shows the theoretical adiabatic flame temperatures obtained for various fuel concentrations through the CANTERA [16] and CAE Run [17] software. The assumed initial reactant temperature was 100 K. This value was chosen because of the limitations in OpenFOAM where any value below 100 K does not get modelled properly and leads to impractical results. The adiabatic flame temperatures are used as reference values against which the temperature values from OpenFOAM simulations are compared to determine whether the temperatures obtained from simulations are practical. All these computed values are for 1 bar pressure.

| **Concentration** | **Adiabatic Flame Temperature (K)** |
|---|---|
| 25% $H_2$ and 75% He | 2720.20 |
| 30% $H_2$ and 70% He | 2765.52 |
| 50% $H_2$ and 50% He | 2946.98 |

| | |
|---|---|
| 75% $H_2$ and 25% He | 3028.99 |
| 90% $H_2$ and 10% He | 3057.93 |
| 95% $H_2$ and 05% He | 3065.71 |
| 100% $H_2$ | 3072.79 |

Table 3.1: Theoretical Adiabatic Flame Temperatures at different helium concentrations

### 3.1 OpenFOAM SIMULATIONS

The major results obtained from the OpenFOAM simulations are temperature and molar concentration profiles. The reactingFoam model in OpenFOAM which incorporates multiphase fluid mechanics with chemical interactions is used to obtain these results.

The energy balance specified in Section 2.9 was satisfied for an oxygen blowing velocity of 0.0853 m/s. This value was applied for all simulations reported here. The hydrogen/helium fuel mixture is input from the right boundary of the computational domain whereas oxygen is input at the left boundary with the specified blowing velocity. Among the other mandatory input parameters required, the pressure for each simulation was specified to be 1 bar and the input temperature was 100 K. Each of the simulations were run for a time of 1 second. Fig. 3.1 shows the plot of temperature v/s time traces for 30% $H_2$ and 70% He for $U$=0.0853 m/s for a six-step chemistry scheme at different points within the computational domain and highlights the reason why all the simulation presented in this chapter were run for a time of 1 sec. These results indicate that the temperature at every point within the computational domain achieves a quasi-steady condition after the time of 0.70 sec. Thus, an elapsed time of 1 second is taken as the quasi-steady flame solution.

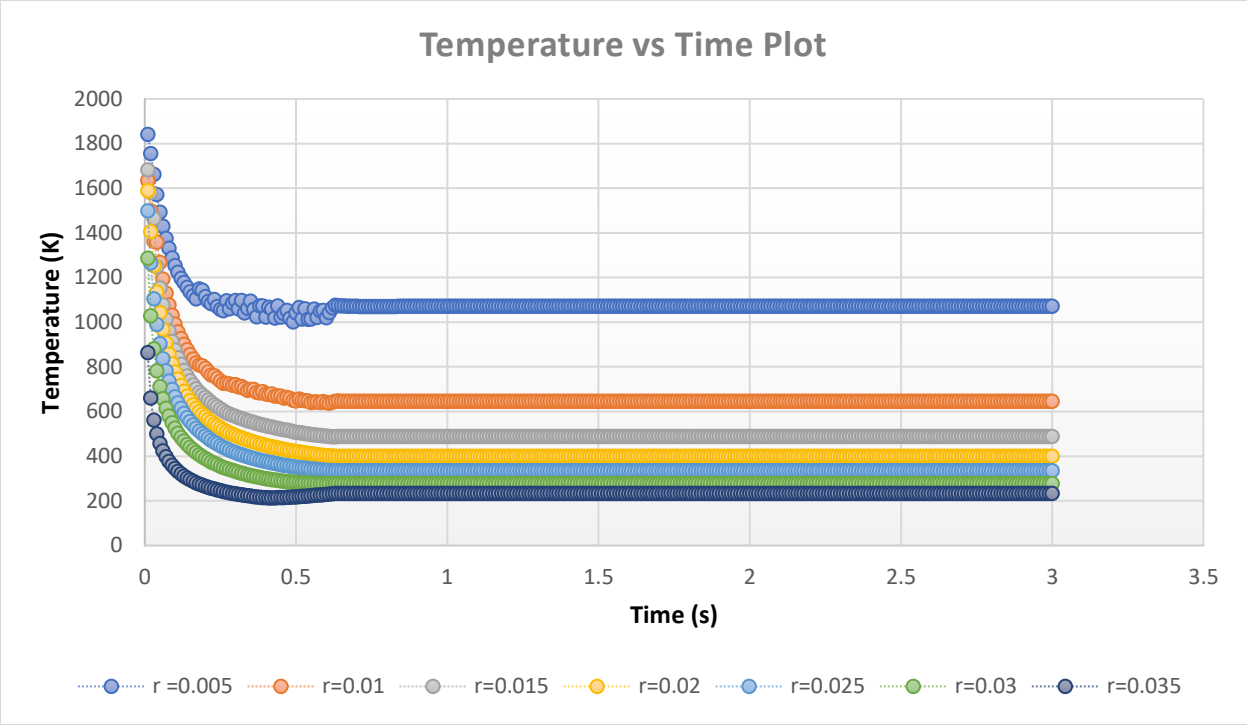


Figure 3.1 Time Evolution of Temperature for 30% $H_2$ and 70% He at U=0.0853 m/s

### *3.1.1 One-Step Chemistry*

Running the OpenFOAM simulations using the chemical scheme specified in section 2.3.1 involving one chemical reaction and three participating species, yields the results for temperature profile and molar species as shown in Figs. 3.2 and 3.3, respectively. All the simulation results presented are for the isothermal wall boundary conditions. Isothermal wall boundary condition is chosen over the adiabatic wall boundary condition as they gave better results. Due to the single-step chemistry, this was the least computationally expensive simulation and hence had the shortest simulation time. The peak flame temperature is 2600 K and the peak water vapor mole fraction at that temperature is close to 0.74. The value of flame temperature agreed reasonably well with the theoretical flame temperature value in Table 3.1. The oxygen species concentration becomes zero after a radial distance of 0.0012 m. The water concentration peaks near the flame front and decreases after that point. Both the hydrogen and helium concentrations continue to decrease rapidly as they approach the droplet surface and eventually become zero.

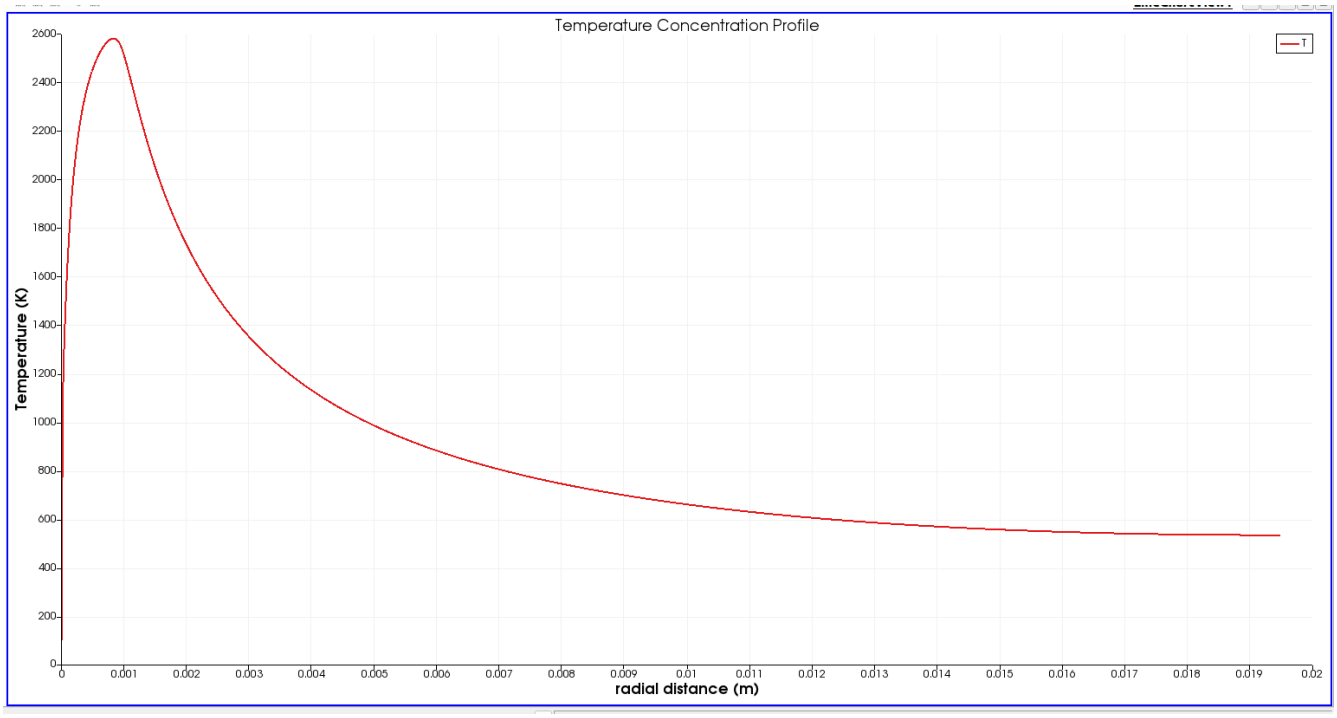


Figure 3.2: Temperature Profile for 30% $H_2$ and 70% He at t=1 sec for one step chemistry

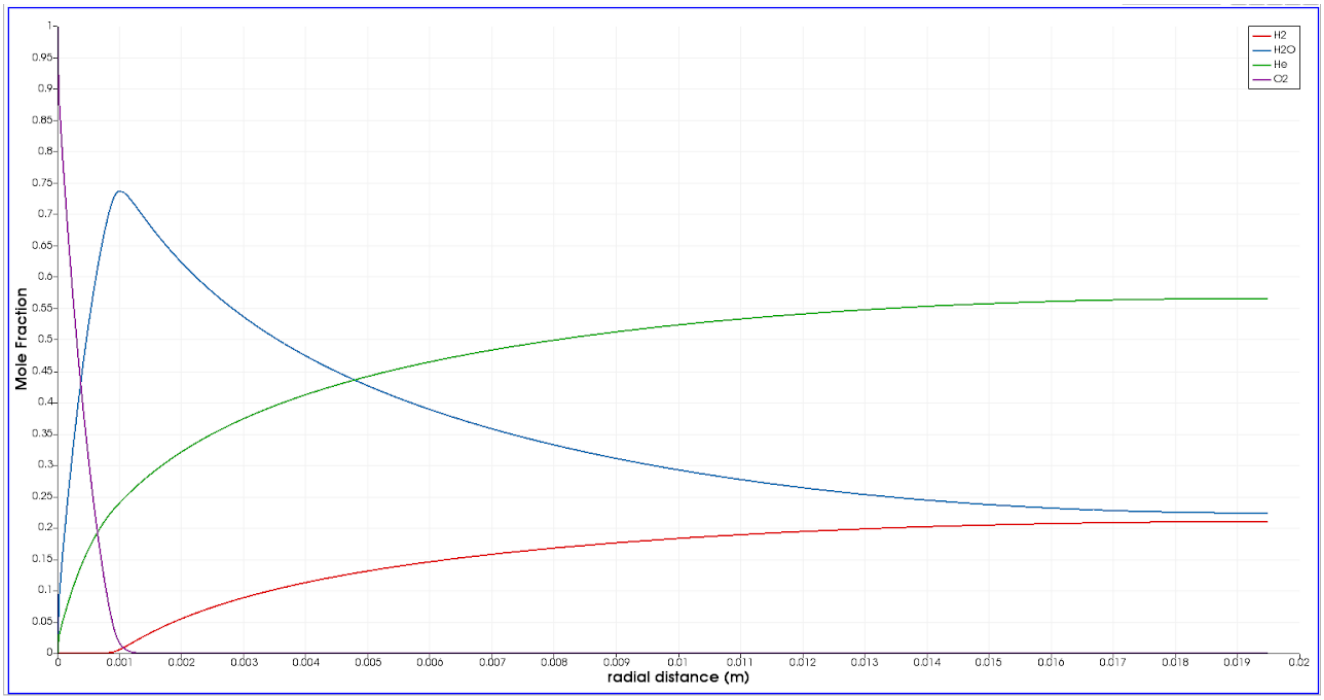


Figure 3.3: Major species profiles for 30% $H_2$ and 70% He at t=1 sec for one step chemistry

For both the species and temperature profile plots shown here, the $x$=0 (the starting point of the computational domain) represents the droplet surface. Once the droplet is ignited using the

superimposed temperature profile, a thin flame zone is formed near the droplet surface. This thin flame zone represents that the comparatively fast chemistry that is expected from the one-step chemistry scheme. This is consistent with the experimental results at ZARM have reported that an ignitable mixture was present very close to the droplet surface [2]. While the experiments have a constant F/D ratio of 2.5 [2], in the numerical model the F/D ratio obtained is close to 1.5. This also validates that reactingFoam solver within the OpenFOAM framework can model the high diffusion of $H_2$ in $O_2$ at the blowing velocity of U=0.0853 m/s with reasonable accuracy. Similar thin-flame zones are also observed for four-step and six-step chemistry.

### *3.1.2 Four-Step Chemistry*

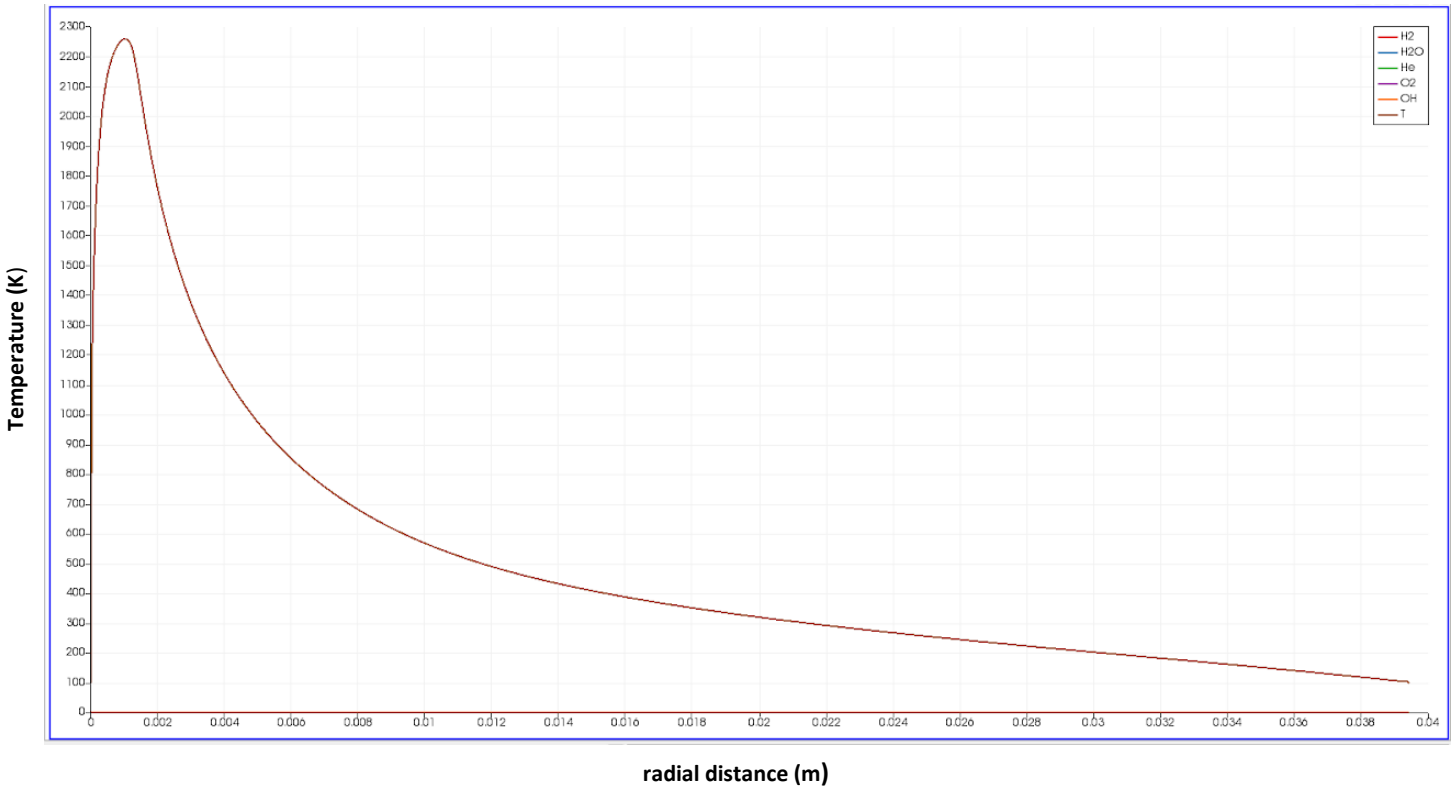


Figure 3.4: Temperature profile for 30% $H_2$ and 70% He at t=1 sec for four step chemistry

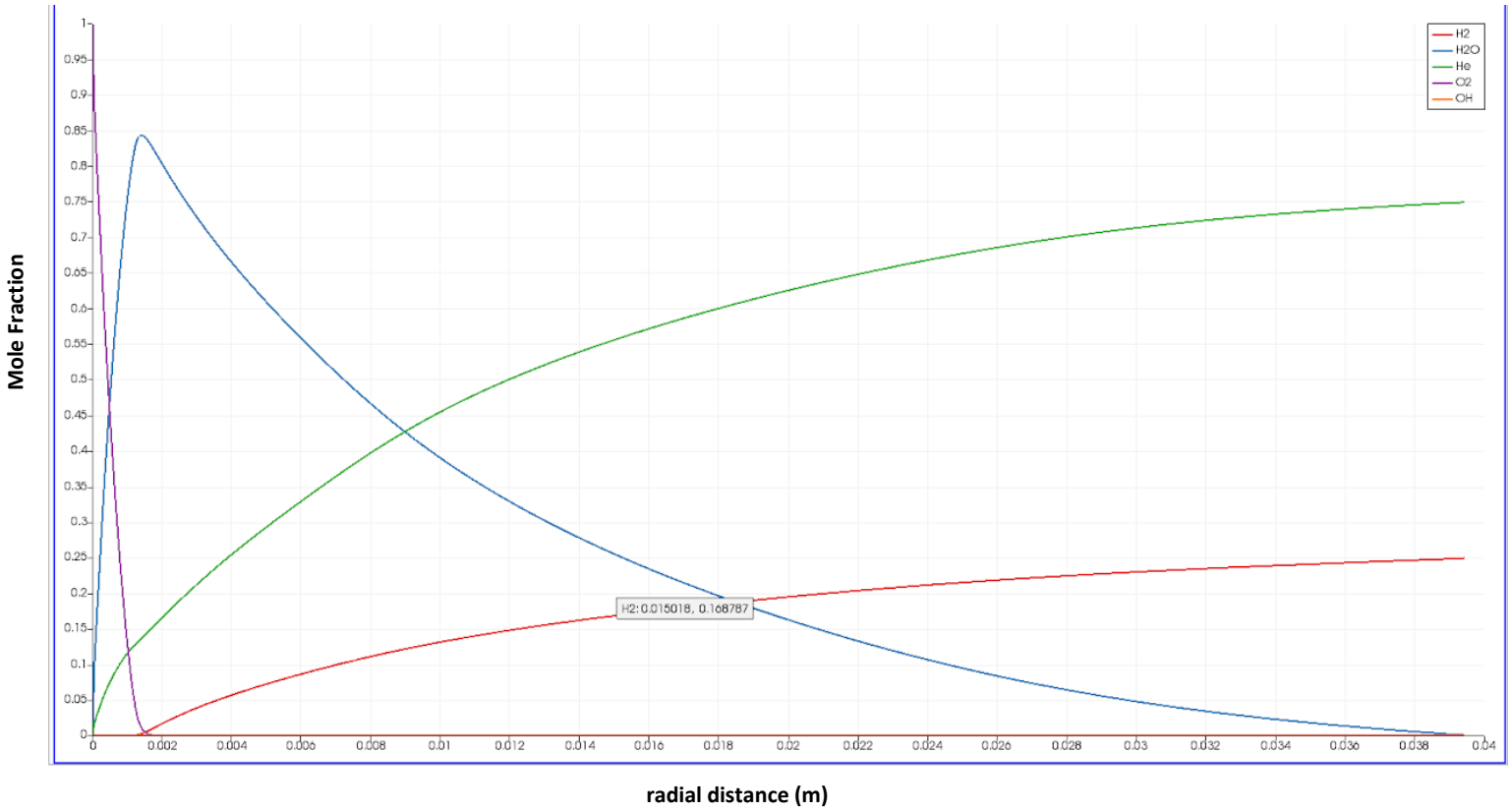


Figure 3.5: Major species profiles for 30% $H_2$ and 70% He at t=1 sec for four step chemistry

Running the OpenFOAM simulations using the chemical scheme specified in Section 2.3.2 involving four-step chemical reactions and six participating species, the results for temperature profile and molar species as shown in Figs. 3.4 and 3.5, respectively, were obtained. Due to the four-step chemistry, this was the more computationally expensive than the one-step chemistry scheme but less computationally expensive than the six-step step chemical scheme. The peak flame temperature is 2300 K and water mole fraction at that temperature is close to 0.85. The oxygen species mole fraction becomes zero after a radial distance of 0.0016 m. The water concentration peaks near the flame front and decreases after that point. Both the hydrogen and helium concentrations continue to decrease rapidly as they approach the droplet surface and eventually become zero. The flame temperature of 2300 K was off by almost 500 K to that of the theoretically

expected flame temperature value of 2765 K. This was surprising as the four-step chemistry does an even worse job in predicting the adiabatic flame temperature value in comparison to the one-step chemistry. This was surprising as it was expected that the four-step chemistry would offer better estimates than the one-step chemistry model which was off only by 200 K.

### *3.1.3 Six-Step Chemistry*

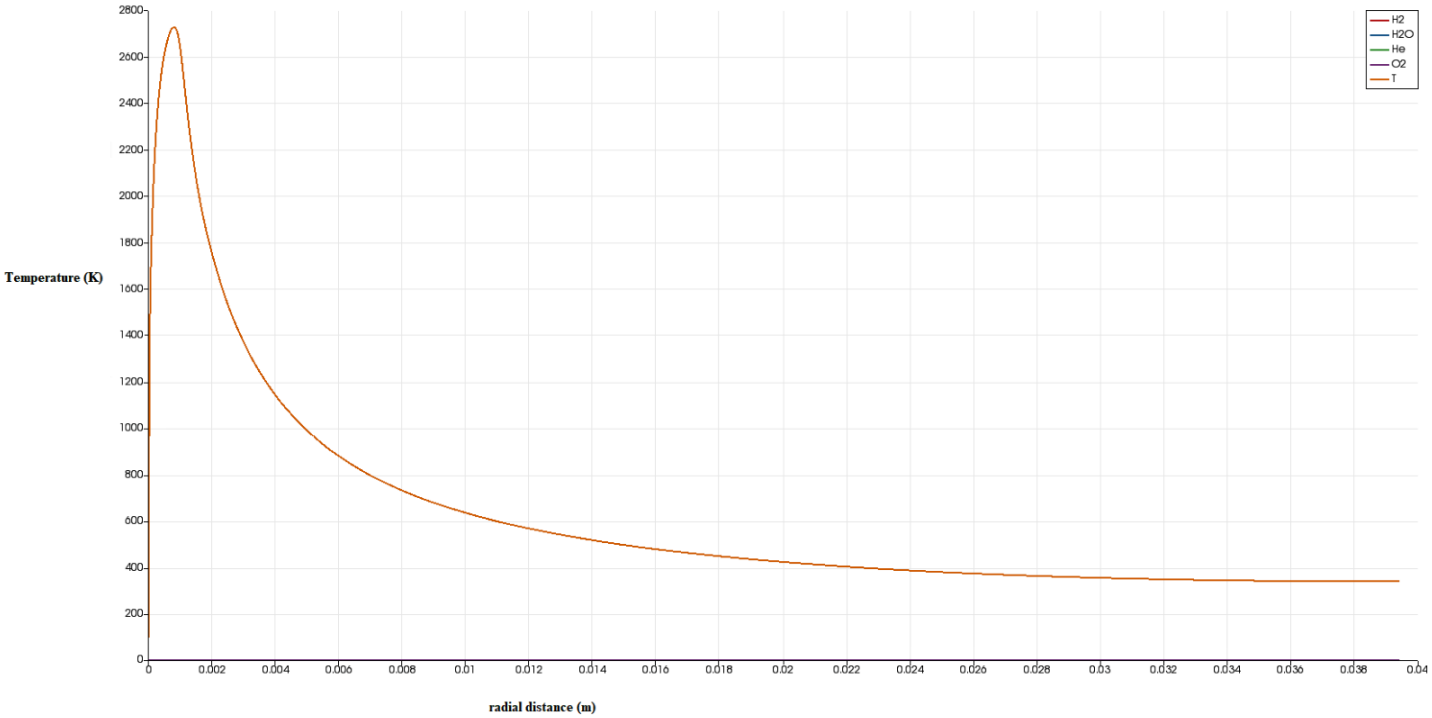


Figure 3.6: Temperature profile for 30% $H_2$ and 70% He at $t$=1 sec for six step chemistry

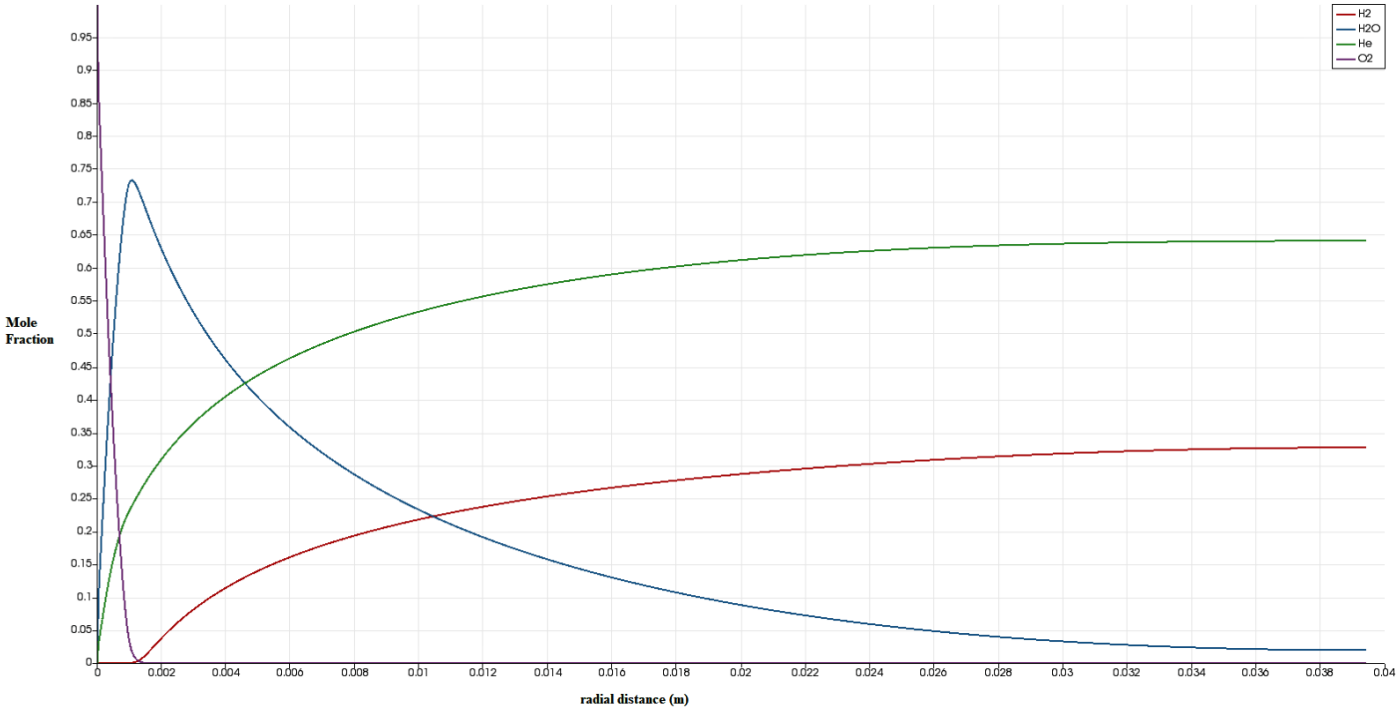


Figure 3.7: Major species profiles for 30% $H_2$ and 70% He at t=1 sec for six step chemistry

Running the OpenFOAM simulations using the chemical scheme specified in Section 2.3.3 involving six chemical reactions and six participating species, the results for temperature profile and molar species as shown in Figs. 3.6 and 3.7, respectively, were obtained. Due to the six-step chemistry, this was the most computationally expensive simulation and hence had the largest simulation computational time. The peak flame temperature is 2760 K and water mole fraction at that temperature is close to 0.74. These values match the expected theoretical results as the theoretical adiabatic flame temperature value obtained was 2765 K. The oxygen species mole fraction becomes zero after a radial distance of 0.0012 m. The water concentration peaks near the flame front and decreases after that point. Both the hydrogen and helium concentrations continue to decrease rapidly as they approach the droplet surface and eventually become zero. Since the flame temperature and species concentration values matched the expected theoretical results, this good agreement formed the basis of utilizing the six-step chemistry scheme as the foundational case for this work.

## 3.2 DROPLET EVAPORATION

The droplet evaporation model specified in Section 2.9 was developed using MATLAB. Based on the results obtained from OpenFOAM simulations, it was determined that a six-step chemistry with a blowing velocity *U*=0.0853 m/s represents the best case to be incorporated into the coupled model. This is achieved by specifying temperature probe within the *controlDict* file in the *reactingFOAM* solver of OpenFOAM. The profile at *r*=0.015 represent the flame front and its average value over 1 second has been used to compute the value of the temperature gradient, $\frac{\partial T}{\partial r}$ . Figure 3.8 shows the water concentration near the droplet surface during the simulation using the theoretical parameters specified in the model as described in the section 2.9. The energy balance which forms the basis of the coupled droplet model is described by Eq. 2.15. This energy balance is satisfied by varying the value of the transfer number $B_q$ in the mass flow rate Eq. 2.16 until the Eq. 2.15 is satisfied. As pointed above, the value of temperature profile $\frac{\partial T}{\partial r}$ is determined from OpenFOAM, and the value of $k_g$ is computed using equation 2.17. The transfer number obtained that satisfies the energy balance equation is 4.4.

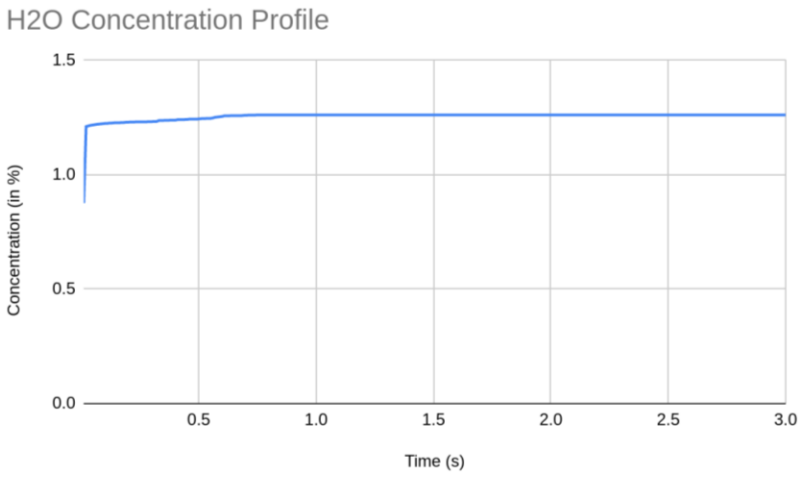


Figure 3.8: Water concentration near the droplet surface

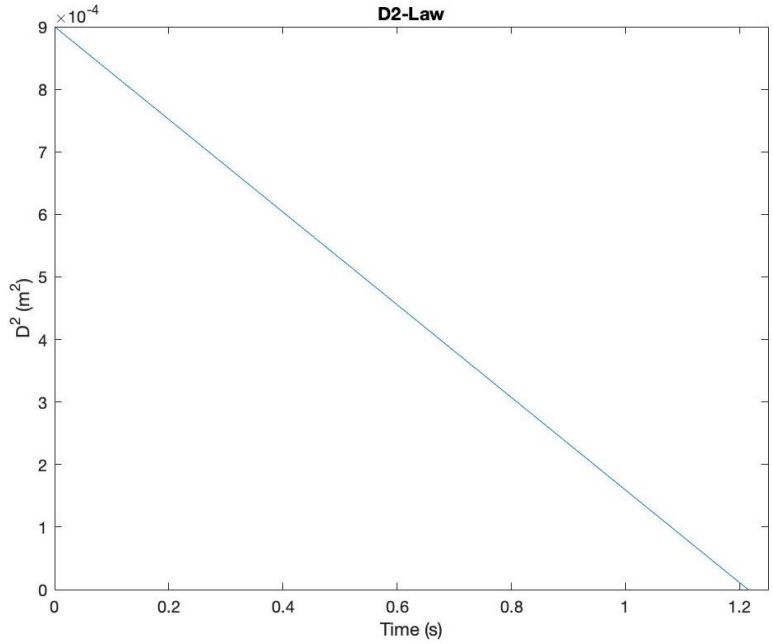


Figure 3.9: $D^2$ Law for the liquid oxygen droplet combustion

The $D^2$ law for the coupled droplet model is evaluated using Eqns. 2.18, 2.19, and 2.20. Once the vaporization rate is computed, the $D^2$ Law is plotted, and estimated droplet lifetime is determined. The OpenFOAM solution does not consider moving-boundary effects, but simply uses the initial condition, combined with the $D^2$ law, to estimate the droplet lifetime. The droplet lifetime is then the time on the $D^2$ Law plot where the line intersects the x-axis. The droplet vaporization rate obtained is $7.4045 * 10^{-4}\ \frac{m^2}{s}$. The droplet lifetime obtained using the coupled model is 1.21 sec. This is an order of magnitude larger than the droplet lifetime of 137 ms observed experimentally [2,3]. Some of the reasons for this difference in results could include the lower thermal conductivity used in the theoretical model in comparison to the experimental setup which uses a suspender to capture the droplet and then ignite it [3]. All these parameters are computed for 30% $H_2$ and not 100% $H_2$. The estimated value of $\frac{\partial T}{\partial r}$ for the 100% $H_2$ condition, based on the corresponding adiabatic flame temperature, is 2000 K/m. The value of $\frac{\partial T}{\partial r}$ obtained from

OpenFOAM which has been selected in the model could also be the reason for this difference. The value of $\frac{\partial T}{\partial r}$ used to perform the calculations using the coupled model is 595.3 K/m. The value of thermal conductivity obtained for 30% $H_2$ with the $\frac{\partial T}{\partial r}$ value of 575.3 K/m is 0.1530 W/mK. Scaling the value of thermal conductivity for 100 % $H_2$ with the value of $\frac{\partial T}{\partial r}$ assumed to be 800 K/m, the value rises to 0.2057 W/mK. Based on these comparisons, we see that the difference in thermal conductivity values for 100 % $H_2$ and 30 % $H_2$ is almost 1.3 times. This partially explains the plausible difference between the experimental and numerical results.

### 3.3 DISCUSSION

From running the simulations in OpenFOAM it was determined that OpenFOAM does adequately provides flame temperature and major species profile concentration for up to 30% $H_2$ fuel diluted with helium. If the concentration exceeds this threshold of 30% $H_2$ and 70% He, the species profiles become impractical as well as the flame temperatures get over-predicted. The primary reason for this deviation appears to be the unity Lewis number assumption in OpenFOAM. If the Lewis number is inaccurate, then the time scales of diffusion process could be mismatched. This is consistent with the unrealistically high flame temperature and hydrogen diffusion at higher hydrogen concentrations and lower flame temperatures and hydrogen diffusion at lower hydrogen concentrations. Determining the heat flux from OpenFOAM simulations and coupled droplet model proved to be challenging. While trying to use paraView to estimate the heat flux associated with the droplet, a surprisingly fixed value of the heat source term, Q, was obtained at all the times for the droplet simulation and for various $H_2$ concentrations. It is unclear what the exact reason for this phenomenon are. One possibility is that the fixed superimposed imposed temperature profile used to ignite the droplet could be the reason for this behavior. Additionally, it is difficult to

estimate the thermal conductivity in the vicinity of the droplet and the theoretical values used in the coupled droplet model for the thermal conductivity might not represent those present physically in the experiments. Also, the value of $\frac{\partial T}{\partial r}$ used to achieve the mass balance in the coupled droplet model could also be lower than the value in the experiment as the experiment considers the value of 100% $H_2$, as discussed previously, whereas the numerical and couped droplet model only considers 30% $H_2$. All these reasons combined could explain the very high value of computed droplet lifetime (1.21 sec in comparison to 136.5 ms observed experimentally). In addition, both OpenFOAM and the coupled droplet model do not account for the apparent and the possible presence of microexplosions which could influence the vaporization rate and the droplet lifetime. Figure 3.10 shows the experimental data of the $D^2$ law and flame standoff distance obtained by our collaborators at ZARM. Here the combustion was conducted at a pressure of 12 bar and the F/D ratio at a pressure of 12 bar is equal to 2.5. The F/D ratio obtained using the numerical model for a pressure of 1 bar is 1.5. Owing to the difference in pressures between the experimental results and the numerical model, the F/D ratio between the two studies does not match.

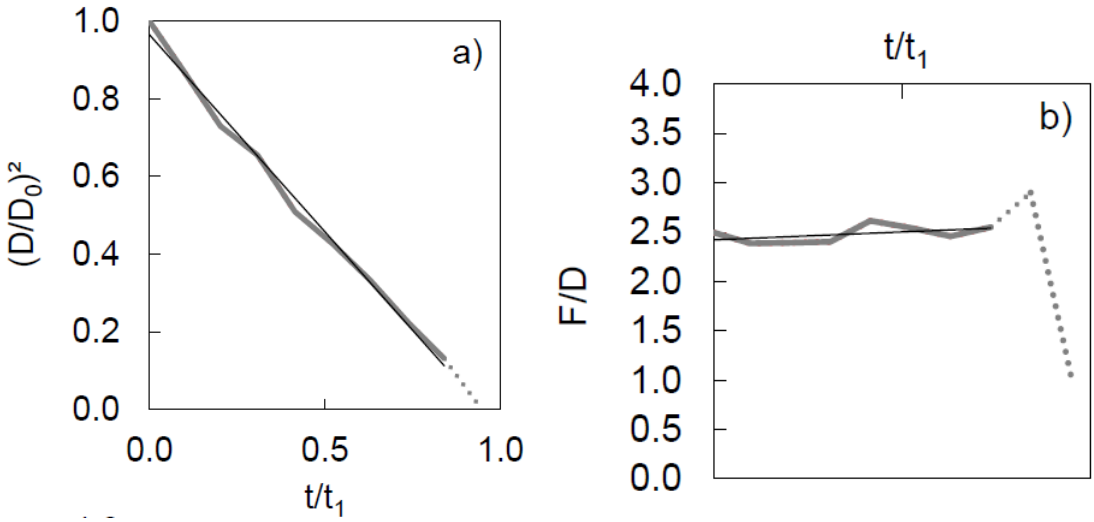


Figure 3.10 Experimental results of combustion at 12 bar after droplet detachment. (a) Droplet diameter regression rate (b) Flame-standoff distances [2]

In addition to these approaches, OpenSMOKE ++ software was also explored to model the LOX oxygen droplet combustion and determine the droplet vaporization rate and the droplet lifetime. OpenSMOKE++ is a software developed by the CRECK Modeling Lab at Politechnico Di Milano [18,19]. The main idea behind using OpenSMOKE++ was to use the microgravity droplet solver inside the OS++ suite and modify it to obtain the desired cryogenic droplet combustion in microgravity. The main difficulty encountered while using this tool was that the solver, still under development, is written for the case of liquid fuel combustion in air. As such, a major limitation of using the solver stems from the fact that it requires dilute nitrogen even to run basic simulations and cannot be extended to model droplet combustion in cryogenic conditions. In addition to microgravity droplet solver, counterFlowFlame1D solver was also explored. This solver also offered similar problems to the microgravity droplet solver when the simulation was run for cryogenic conditions. The software crashed without providing an output. Based on these findings, the author decided not to pursue this approach.

# CHAPTER 4

# CONCLUSIONS

Based on the numerical and coupled Droplet Evaporation model, the following results were obtained:

- The concentration of 30% $H_2$ and 70% He was identified as the limiting case for running simulations of oxygen combustion in OpenFOAM under cryogenic conditions. For this fuel composition, the adiabatic flame temperature matches the results from CANTERA and CAE Run with a physically reasonable helium diluent concentration. For concentrations above 30% $H_2$, an unreasonable increase in the value of He concentration is observed in the middle of the computational domain. This renders the results obtained above this concentration to be impractical and unreasonable.
- A oxygen blowing velocity of 0.0853 m/s satisfied the necessary mass/energy balance as the simulated droplet surface.
- Six-step chemistry appears to work best for modeling the cryogenic droplet combustion of liquid oxygen droplet in microgravity conditions as the temperature and best matches the theoretical values. Four-step chemistry and one-step chemistry do not model the problem accurately and under-predict the value of adiabatic flame temperature. Another issue associated with one-and four-step chemistry is the observation of a spike in the helium concentration in the middle of the computational domain at higher concentrations which is unphysical. In addition, for the four-step chemistry the values of Arrhenius equation pre-exponential A, Temperature exponential of the modified Arrhenius equation β, and Activation Energy Ta are not available in the literature

- The simulations were run for a time of 1 sec as the temperature profile become steady at throughout in the computational domain
- Unity Lewis Number assumption in OpenFOAM appears to over-predict the adiabatic flame temperature. This becomes especially prevalent at higher hydrogen concentrations where a difference of more than 500 K was observed in some cases
- A Coupled droplet model is used to determine the droplet vaporization rate, droplet lifetime, and plot the $D^2$ Law. A droplet lifetime of 1.21 sec is obtained using the coupled droplet model. The droplet lifetime obtained using the coupled model is an order of magnitude greater than the value obtained experimentally. This can be accounted for by the smaller temperature and lower value of thermal conductivity compared to the case of pure hydrogen.
- OpenSMOKE++ developed by researchers at Politecnico Di Milano does not model the problem of cryogenic droplet combustion of liquid oxygen droplet in microgravity conditions

# CHAPTER 5

# RECOMMENDATIONS AND FUTURE WORK

Based on the findings of this work, the following are suggested for future research:

- OpenFOAM in its current capabilities does not model the problem of cryogenic combustion of liquid oxygen droplet in microgravity conditions owing to its unity Lewis number assumptions. There is a need to develop a solver within the OpenFOAM framework which bypasses this unity Lewis number assumption which will aide in achieving modelling of higher hydrogen concentration without seeing impractical temperature profiles.
- Based on a recent literature review, the author came across a solver named "reactingLeFOAM" [20] which is an OpenFOAM solver eliminating the unity lewis number assumption. This solver could help in removing the exisiting modelling limitations experienced with OpebFOAM and help in understanding better the root cause of impractical temperature and He molar concentration profiles.
- Modifying and implementing the existing numerical model developed for the liquid fuel droplet combustion by our collaborators at ZARM to model the combustion of liquid oxygen droplet is another approach which will be undertaken in the future work. Preliminary work to achieve this has already started.
- Future models could consider the cases of radiation, turbulence, and surface tension as it might provide a better insight into the droplet combustion physics.

- A future study with the four-step chemistry scheme could also be implemented with the known and correct values of Arrhenius equation pre-exponential A, Temperature exponential of the modified Arrhenius equation β, and Activation Energy Ta.

## REFERENCES

[1] http://www.braeunig.us/space/propel.htm

[2] Meyer, F., Eigenbrod, C., Wagner, V., Paa, W., Hall, J.D., Zody, M., Frydman, J., and Hermanson, J.C, "Combustion of Single Oxygen Droplets in Hydrogen Under Microgravity Conditions", The 31st International Symposium on Transport Phenomena, 13-16 October 2020, Honolulu, USA

[3] Meyer, F., Eigenbrod, C., Wagner, V., Paa, W., Hall, J.D., Zody, M., Frydman, J., and Hermanson, J.C. "Combustion of Single Oxygen Droplets in Hydrogen Under Microgravity Conditions." In *AIAA Scitech 2021 Forum*. American Institute of Aeronautics and Astronautics. doi:10.2514/6.2021-0548.

[4] Meyer, F., Eigenbrod, C., Hermanson, J.C., Frydman, J., Paa, W., and Wagner, V., "Microgravity Experiments and Numerical Simulations on the Combustion of Single Oxygen Droplets in Hydrogen*," 69th International Astronautical Congress (IAC)*, Bremen, Germany, October 2018.

[5] Hermanson, J.C. *et al,* "Numerical Simulation of Liquid Oxygen Droplet Combustion in Hydrogen", 72nd Annual Meeting of the APS Division of Fluid Dynamics, Vol. 64 no.13, (2019)

[6] Greenshields, C.J., OpenFOAM Programmer's Guide version 5.0. OpenFOAM Foundation Ltd., 2017.

[7] https://www.openfoam.com/documentation/user-guide

[8] P.J. Linstrom and W.G. Mallard, Eds., **NIST Chemistry WebBook, NIST Standard Reference Database Number 69**, National Institute of Standards and Technology, Gaithersburg MD, 20899, https://doi.org/10.18434/T4D303, (retrieved June 3, 2021).

[9] Irvin Glassman and Richard A. Yetter. Combustion. Academic Press, Oxford, 4 edition,2008

[10] Peter Kidwelly, editor. Detailed and Global Chemical Kinetics Model for Hydrogen. Lawrence Livermore National Lab., CA, 1995.

[11] Boivin, Pierre & Jiménez, C. & Sánchez, A. and Williams, F., "An explicit reduced mechanism for H2–air combustion," Proceedings of the Combustion Institute, Vol. 33, pp. 517-523, (2011). 10.1016/j.proci.2010.05.002.

[12] Doubiani, N.: A NOx model tutorial. In Proceedings of CFD with OpenSource Software, 2019, Edited by Nilsson. H., http://dx.doi.org/10.17196/OS_CFD#YEAR_2019

[13] Frydman, J., "Transient Oxygen Droplet Combustion in a Hydrogen Atmosphere: A Numerical Approach". M.Sc. thesis, University of Washington, Seattle, USA, 2018.

[14] Turns, S.R., A*n introduction to combustion* (2nd Edition), McGraw-Hill, 2000.

[15] Bird, R.B., Stewart, W.E., and Lightfoot, E.N., *Transport Phenomena*, Wiley, New York, 1960.

[16] Goodwin, D.G., Speth, R.L., Moffat, H.K. and Weber, B.W. *Cantera: An object-oriented software toolkit for chemical kinetics, thermodynamics, and transport processes*. https://www.cantera.org, 2021. Version 2.5.1. doi:10.5281/zenodo.4527812

[17] Gordon S., McBride B.J. **Computer program for calculation of complex chemical equilibrium compositions and applications: I. Analysis: Tech. Rep. RP 1311**. NASA (1994)

[18] Cuoci, A., Frassoldati, A., Faravelli, T., and Ranzi E., "OpenSMOKE++:An object-oriented frame-work for the numerical modeling of reactive systems with detailed kinetic mechanisms," *Computer Physics Communications*, Vol. 192, p.237-264 (2015), DOI:10.1016/j.cpc.2015.02.014

[19] Cuoci, A., Frassoldati, A., Faravelli, T., and Ranzi E., "A computational tool for the detailed kinetic modeling of laminar flames: Application to C2H4/CH4 coflow flames," *Combustion and Flame*, Vol. 160 (5), p.870-887 (2013), DOI: 10.1016/j.combustionflame2013.01.011

[20] Bulut Tekgul, reactingLeFOAM, https://github.com/blttkgl/reactingLeFoam

# APPENDIX A

## A.1 MATLAB Code for the coupled Droplet Model

```
clc;
clear all;
%% Coupled MATLAB OpenFOAM model

%Step 1: Pick a velocity of U
U=0.0853; %in m/s

%Step 2: Select the best concentration profile and chemistry scheme
%Profile concentration selected is 30% H2 and 70% He and six step chemistry
scheme

%Step 3: Obtain the temperature and concentration profiles from OpenFOAM

%Step 4: Obatin dT/dr from OpenFOAM
dT_dr= 595.3; %in K

%Step 5: Determine the value of thermal conductivity k near the droplet
surface using profile from OpenFOAM and bird's model
Cp_birdforth= 0.00025706952; %in KJ/kg*K.

%Step 6: Calculate Cp*dt_dr
Kappa_birdforth= Cp_birdforth*dT_dr;

%Step 7: Compute the desired parameters
h_fg= 271.013;%in KJ/kg (213)
rs= 0.015;%in m
m_dot_birdforth= Kappa_birdforth*dT_dr*4*pi*rs^2/h_fg;

%Step 8: Compute U
rho_l=3.941; %in kg/m3
U_new= m_dot_birdforth/((4*pi).*(rs.^2)*rho_l);

%Step 9: Determine kg
kg= m_dot_birdforth*h_fg/(4*pi*dT_dr*rs^2);

%Step 10: Determine the transfer number
c_pg= 1.850; %in kJ/kg*K
Bq=1+ exp(m_dot_birdforth*c_pg/(4*pi*kg*rs));

%Step 11: Determine the evaporation constant
rho_l= 1000; % Density of water in kg/m3
K= 8*kg*log(Bq+1)/(rho_l*c_pg);

%Step 12: Compute the D2 Law and plot it
t= 0:0.01:1.23;
D_squared_t= 4*rs^2- K*t;
td= 4*rs^2/K; % droplet lifetime (s)
plot(t,D_squared_t)
xlim([0 1.25])
```

```
ylim([0 9*10^-4])
ylabel("D^2 (m^2)")
xlabel("Time (s)")
title("D2-Law")
```